

Bidirectional emission from a ring resonator driven by an external field and containing a saturable absorber

Zongxiong Ye and Lorenzo M. Narducci

Department of Physics, Drexel University, Philadelphia, Pennsylvania 19104

(Received 19 October 2000; published 16 March 2001)

We formulate a first-principles description of the behavior of a bidirectional ring cavity containing a saturable absorbing medium, and driven by an external coherent field. The setting of interest to this study is an extension of the ordinary optically bistable system, where a ring resonator supports only one of the two possible directions of propagation of the cavity field. In this more general case and in the uniform-field limit, we show that the dynamics of the fields-atoms system is described by an infinite set of coupled equations that can be readily solved by standard numerical means after appropriate truncation of the number of atomic variables. With the help of two different approaches, we find unexpected, long-time stationary solutions such that the forward and backward fields oscillate with different carrier frequencies: the first is based upon the time-dependent equations and the second on a set of nonlinear-algebraic equations describing the steady states. As an added confirmation, we carry out a linear-stability analysis of the unidirectional steady state for the purpose of identifying the conditions under which a backward field can grow from an initial fluctuation. By this approach we also suggest a possible strategy for the experimental observation of stationary, frequency-shifted output fields.

DOI: 10.1103/PhysRevA.63.043815

PACS number(s): 42.65.Pc, 42.65.Sf, 42.55.Ah

I. INTRODUCTION

Bidirectional ring resonators have played a significant role in laser physics and quantum optics [1]. An extensive literature deals with theoretical and experimental aspects of the behavior of bidirectional ring cavities containing an active medium [2]. In contrast, much less attention has been paid to the counterpart problem of a bidirectional resonator containing a passive medium and driven by an external coherent field. Of course, this comment does not include cavities configured as Fabry-Perot resonators where bidirectional propagation is an unavoidable consequence of the geometry of the mirrors [3].

In fact, an extensive amount of work during the mid 1970s and early 1980s dealt with the bistable properties of ring cavities containing a passive medium but, for the most part, these studies focused on a setting where the cavity could support only unidirectional propagation in the same direction as the external field [3,4]. And, indeed, this has been largely the outcome of experiments, as reported for example by Kimble and collaborators [5]. Exceptions were noted but, to our knowledge, they were not investigated further [6].

In a significant contribution that appears to have attracted only limited attention, Asquini and Casagrande [7] investigated the bistable properties of a bidirectional ring cavity under resonance conditions, i.e., when the frequency of the driving field matches the frequency of one of the cavity modes and the atomic transition frequency. They studied the steady-state behavior and the linear stability of the system around steady state, and concluded that bidirectional propagation does not introduce novel stationary features, relative to the unidirectional case. Their linear stability analysis, instead, suggested the existence of instabilities in the counter-propagating field, in addition to the known self-oscillations of the forward field.

The purpose of this paper is to reexamine the conclusions of Ref. [7] in the more general setting involving arbitrary detuning parameters, and to propose the existence of an unexpected steady state in which both forward and backward fields emerge from the resonator with slightly different carrier frequencies. To be more precise, we predict that in steady state the forward field oscillates in synchronism with the injected field, while the backward field is frequency shifted from both. This is surprising because, at first sight, one would not expect a steady state if the forward and backward fields oscillate with different frequencies in the same optical resonator.

We derive our working equations following a somewhat different procedure from the one used in Ref. [7], and introduce a version of the boundary conditions that, upon suitable change of the field variables, can be cast into the standard periodic form appropriate for an ideal resonator. In terms of the new variables, the equations of motion acquire the expected field damping terms, and terms containing the cavity-mistuning parameter. The advantage of our approach is that, in the uniform-field limit, it can readily yield information not only on the steady-state properties of the system, but also on its transient evolution with the help of standard numerical methods.

We find ourselves in agreement with the conclusions reached by Asquini and Casagrande under resonance conditions. However, in the more general setting in which arbitrary detuning parameters are allowed, a backward field with a nonzero, time-independent amplitude can coexist with a stationary forward field, provided that its carrier frequency is different.

With regard to the physical interpretation of this effect, we believe that the following sequence of events is likely to play a role in this unusual phenomenon: the backward wave grows from spontaneous emission noise; its gain is provided by an initially small fraction of the forward wave that is

Bragg-scattered from the atomic polarization and population gratings formed in the medium by the interference between the counterpropagating components. When the gain of the backward wave exceeds the cavity losses, a steady-state condition is eventually reached in which the backward field operates, in essence, as a ring laser of its own, subject to its own boundary conditions. In fact, the value of the frequency shift, calculated numerically, is often well approximated by the usual mode-pulling formula of ordinary-laser theory.

We have calculated the stationary fields and their frequency difference by solving the time-dependent equations of the system for long times and, independently, also by solving the nonlinear-algebraic equations that describe the steady-state configurations. These results, not surprisingly, are in excellent agreement with each other and offer mutual support in favor of the existence of the frequency-shifted steady states.

As an additional independent check, we have also carried out a linear-stability analysis in the neighborhood of steady states with zero backward field, and determined the parameters that favor the growth of an initial backward field fluctuation. The boundaries of these unstable domains are in excellent agreement with those derived from the time-dependent equations and from their stationary counterparts.

Our paper is organized as follows. Section II contains a description of the model and a derivation of the equations of motion, ending with the infinite set of working equations in the uniform field limit. In Sec. III we discuss two possible kinds of steady states. The first, in which the backward field oscillates synchronously with the forward field, is physically unrealizable, as we show. The second class of steady states, characterized by forward and backward fields with different carrier frequencies, is consistent, instead, with the working equations. In this case we derive numerically and display the values of the relevant variables for selected parameters, using an appropriate nonlinear algebraic set of steady-state equations. Section IV describes time-dependent solutions with special emphasis on two sets of system parameters. In Sec. V, we consider the linearized behavior of our system in the neighborhood of steady-state configurations in which only the forward field is nonzero, and determine the conditions that favor the growth of a backward field. Finally, we conclude the paper, in Sec. VI, with a brief overview of our results.

II. DESCRIPTION OF THE MODEL AND EQUATIONS OF MOTION

We consider a ring cavity composed of three mirrors; one is an ideal reflector and the other two have equal power reflectivities, $R < 1$, as shown schematically in Fig. 1. The total length of the resonator is Λ . Inside the cavity, a region of length L is filled with a homogeneously broadened, passive medium made up of two-level atoms. A coherent field is injected into the cavity through one of the two partially transmitting mirrors, while a fraction of the cavity field escapes in both the forward and backward directions [8]. We analyze this model within the plane wave and slowly varying amplitude approximations.

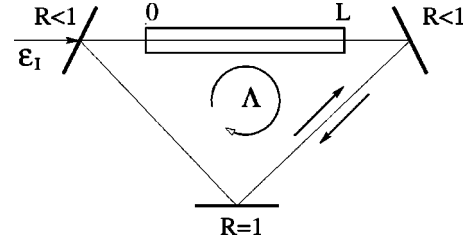


FIG. 1. Schematic representation of the bidirectional ring resonator. The input and output mirrors have equal power reflectivities, $R < 1$, while the third mirror is assumed to be an ideal reflector. The full length of the resonator is Λ , the passive medium is confined to the segment $0 \leq z \leq L$, and E_I denotes the injected field.

We assume the injected signal to be a monochromatic plane wave of the form

$$E_I(z, t) = E_I e^{i(kz - \omega t)} + \text{c.c.}, \quad (1)$$

where E_I is a constant amplitude and ω and $k = \omega/c$ are chosen as the reference frequency and wave number, respectively. As usual, the cavity field $\mathcal{E}(z, t)$ and the macroscopic atomic polarization $\mathcal{P}(z, t)$ are linked by Maxwell's wave equation

$$\left(\frac{\partial^2}{\partial t^2} - c^2 \frac{\partial^2}{\partial z^2} \right) \mathcal{E}(z, t) = - \frac{1}{\epsilon_0} \frac{\partial^2}{\partial t^2} \mathcal{P}(z, t). \quad (2)$$

We assume the cavity field to have the form

$$\mathcal{E}(z, t) = \mathcal{E}_F(z, t) + \mathcal{E}_B(z, t), \quad (3a)$$

where

$$\mathcal{E}_F(z, t) = E_F(z, t) e^{i(kz - \omega t)} + \text{c.c.}, \quad (3b)$$

$$\mathcal{E}_B(z, t) = E_B(z, t) e^{-i(kz + \omega t)} + \text{c.c.}, \quad (3c)$$

and F and B label the forward and backward directions of propagation, respectively. Because we have in mind a near-resonant interaction between the injected field and the atoms, through the intermediary of the cavity field, the amplitudes $E_F(z, t)$ and $E_B(z, t)$ are slowly varying with respect to both z and t . In this way, we can interpret the cavity field $\mathcal{E}(z, t)$ as the superposition of two contributions that propagate in opposite directions with slowly varying amplitudes.

For the macroscopic polarization we assume the representation

$$\mathcal{P}(z, t) = \mu [P^{(+)}(z, t) e^{-i\omega t} + P^{(-)}(z, t) e^{i\omega t}], \quad (4)$$

where μ is the modulus of the atomic transition dipole moment, and $P^{(\pm)}(z, t)$ are slowly varying functions of time but rapidly varying functions of space; moreover, we have $P^{(-)} = [P^{(+)}]^*$.

Upon substituting Eqs. (3) and (4) into Eq. (2), the slowly varying amplitude approximation yields two separate equations for the forward and backward field amplitudes of the form [9],

$$\left(\frac{\partial}{\partial t} + c \frac{\partial}{\partial z}\right) E_F(z, t) = i \frac{\omega \mu}{2 \epsilon_0} \frac{1}{\lambda} \int_z^{z+\lambda} dz' e^{-ikz'} P^{(+)}(z', t), \quad (5a)$$

$$\left(\frac{\partial}{\partial t} - c \frac{\partial}{\partial z}\right) E_B(z, t) = i \frac{\omega \mu}{2 \epsilon_0} \frac{1}{\lambda} \int_z^{z+\lambda} dz' e^{ikz'} P^{(+)}(z', t), \quad (5b)$$

where $\lambda = 2\pi/k$. Note that the slowly varying amplitudes of the cavity field are driven by the local average of the rapidly varying polarization amplitude $P^{(+)}(z, t)$ weighted by the exponential factors e^{-ikz} and e^{ikz} , respectively.

The evolution of the medium is described by the optical Bloch equations after neglecting terms that oscillate at frequencies $\pm 2\omega$ and higher. After inclusion of the usual phenomenological damping terms, the atomic equations have the form

$$\frac{\partial}{\partial t} P^{(+)}(z, t) = -\gamma_{\perp} (1 + i\delta_0) P^{(+)}(z, t) - i \frac{\mu}{\hbar} D(z, t) \times [E_F(z, t) e^{ikz} + E_B(z, t) e^{-ikz}], \quad (6a)$$

$$\frac{\partial}{\partial t} D(z, t) = -\gamma_{\parallel} [D(z, t) - D^{eq}] + 2i \frac{\mu}{\hbar} \{P^{(-)}(z, t) \times [E_F(z, t) e^{ikz} + E_B(z, t) e^{-ikz}] - \text{c.c.}\}, \quad (6b)$$

where γ_{\perp} and γ_{\parallel} are the relaxation rates of the polarization and population difference, respectively, $\delta_0 = (\omega_0 - \omega)/\gamma_{\perp}$, ω_0 is the atomic transition frequency, $D(z, t)$ is the difference between the number densities of excited and ground state atoms, and D^{eq} is the value of D in the absence of the cavity field.

In view of the geometry of the resonator (Fig. 1), the forward and backward fields obey the boundary conditions

$$\mathcal{E}_F(0, t) = \sqrt{T} \mathcal{E}_I(0, t) + R \mathcal{E}_F(\Lambda, t), \quad (7)$$

$$\mathcal{E}_B(\Lambda, t) = R \mathcal{E}_B(0, t), \quad (8)$$

which, in view of Eqs. (3b), (3c), and (1), imply

$$E_F(0, t) = \sqrt{T} E_I + R E_F(\Lambda, t) e^{-i\delta_c}, \quad (9a)$$

$$E_B(\Lambda, t) = R E_B(0, t) e^{-i\delta_c}, \quad (9b)$$

where T is the power transmittivity of the mirrors ($T = 1 - R$), $\delta_c = (\omega_c - \omega)\Lambda/c$ is the cavity mistuning parameter, and ω_c denotes the cavity resonance frequency that is nearest to the carrier frequency of the injected field.

Equations (5) and (6), plus the boundary conditions (9) and appropriate initial conditions, are sufficient, in principle, to analyze the space-time evolution of the bidirectional ring resonator. At this level of generality, the problem is clearly very complex. It is possible to introduce significant simplifications without omitting essential physical aspects if we limit our considerations to the so-called uniform-field limit (UFL) [4,10,11], a situation where the mirrors' transmittivity is reduced in step with the medium absorption coefficient

and the cavity mistuning parameter until the slow spatial variation of the field amplitudes $E_F(z, t)$ and $E_B(z, t)$ becomes almost negligible over a single pass through the medium.

The first step in this program is to introduce new scaled variables, $Y_F(z, t)$ and $Y_B(z, t)$, whose boundary conditions have the standard periodic form of an ideal resonator. The required transformations are

$$E_F(z, t) = \frac{\hbar}{2\mu} (\gamma_{\parallel} \gamma_{\perp})^{1/2} \left(Y_F(z, t) - \frac{z}{\Lambda} |\ln R| Y_I \right) \times \exp \left[-\frac{z}{\Lambda} \ln(R e^{-i\delta_c}) \right], \quad (10a)$$

$$E_B(z, t) = \frac{\hbar}{2\mu} (\gamma_{\perp} \gamma_{\parallel})^{1/2} Y_B(z, t) \exp \left[\frac{z - \Lambda}{\Lambda} \ln(R e^{-i\delta_c}) \right], \quad (10b)$$

where

$$Y_I = \frac{2\mu}{\hbar} (\gamma_{\parallel} \gamma_{\perp})^{-1/2} \frac{\sqrt{T E_I}}{|\ln R|}. \quad (11)$$

In terms of the new field amplitudes, the boundary conditions (9) take the form

$$Y_F(0, t) = Y_F(\Lambda, t), \quad (12a)$$

$$Y_B(\Lambda, t) = Y_B(0, t), \quad (12b)$$

which are, indeed, formally appropriate for an ideal bidirectional ring cavity. Of course, Eqs. (12) do not imply that we are neglecting the cavity damping mechanism or, for that matter, the driving action of the injected field. In fact, as shown below, these contributions appear explicitly in the transformed equations.

Before deriving the new equations of motion, it is also convenient to introduce the scaled atomic variables

$$p(z, t) = \frac{2i}{N} \left(\frac{\gamma_{\perp}}{\gamma_{\parallel}} \right)^{-1/2} P^{(+)}(z, t), \quad (13a)$$

$$d(z, t) = D(z, t)/N, \quad (13b)$$

where N is the number density of atoms. At this point, the equations of motion, in terms of the new variables, take the form

$$\begin{aligned} & \left(\frac{\partial}{\partial t} + c \frac{\partial}{\partial z}\right) Y_F(z, t) \\ &= \frac{c |\ln R|}{\Lambda} Y_I - \frac{c}{\Lambda} \ln(R e^{-i\delta_c}) \frac{z |\ln R|}{\Lambda} Y_I + \frac{c}{\Lambda} \ln(R e^{-i\delta_c}) Y_F \\ &+ c \alpha \exp \left[\frac{z}{\Lambda} \ln(R e^{-i\delta_c}) \right] \frac{1}{\lambda} \int_z^{z+\lambda} dz' e^{-ikz'} p(z', t), \end{aligned} \quad (14a)$$

$$\begin{aligned} & \left(\frac{\partial}{\partial t} - c \frac{\partial}{\partial z} \right) Y_B(z, t) \\ &= \frac{c}{\Lambda} \ln(R e^{-i\delta_c}) Y_B + c \alpha \exp \left[-\frac{z-\Lambda}{\Lambda} \ln(R e^{-i\delta_c}) \right] \\ & \quad \times \frac{1}{\lambda} \int_z^{z+\lambda} dz' e^{ikz'} p(z', t), \end{aligned} \quad (14b)$$

$$\frac{\partial}{\partial t} p(z, t) = -\gamma_{\perp} (1 + i\delta_0) p + \gamma_{\perp} \beta d, \quad (14c)$$

$$\frac{\partial}{\partial t} d(z, t) = -\gamma_{\parallel} (d - d^{eq}) - \frac{1}{2} \gamma_{\parallel} (\beta p^* + \text{c.c.}), \quad (14d)$$

where $\alpha = N\omega\mu^2/2\epsilon_0\hbar\gamma_{\perp}c$ is the unsaturated field absorption coefficient per unit length, $d^{eq} = D^{eq}/N$, and

$$\begin{aligned} \beta &= e^{ikz} \exp \left[-\frac{z}{\Lambda} \ln(R e^{-i\delta_c}) \right] \left(Y_F - \frac{z|\ln R|}{\Lambda} Y_I \right) \\ &+ e^{-ikz} \exp \left[\frac{z-\Lambda}{\Lambda} \ln(R e^{-i\delta_c}) \right] Y_B. \end{aligned} \quad (15)$$

In spite of the significant increase in formal complexity, Eqs. (14) are ideally suited for the implementation of the uniform-field limit. Specifically, we assume the conditions

$$\alpha L \ll 1, \quad T \ll 1, \quad \delta_c \ll 1, \quad (16)$$

subject to the constraints

$$\frac{\alpha L}{|\ln R|} \approx \frac{\alpha L}{T} \equiv 2C = \text{finite number}, \quad (17a)$$

$$\frac{\delta_c}{|\ln R|} \approx \frac{\delta_c}{T} \equiv \theta = \text{finite number}. \quad (17b)$$

With the help of Eqs. (16) and (17), Eqs. (14) take the approximate form

$$\begin{aligned} & \left(\frac{\partial}{\partial t} + c \frac{\partial}{\partial z} \right) Y_F = -\kappa(1 + i\theta) Y_F + \kappa Y_I + \kappa 2C \frac{\Lambda}{L} \frac{1}{\lambda} \\ & \quad \times \int_z^{z+\lambda} dz' e^{-ikz'} p(z', t), \end{aligned} \quad (18a)$$

$$\begin{aligned} & \left(\frac{\partial}{\partial t} - c \frac{\partial}{\partial z} \right) Y_B = -\kappa(1 + i\theta) Y_B + \kappa 2C \frac{\Lambda}{L} \frac{1}{\lambda} \\ & \quad \times \int_z^{z+\lambda} dz' e^{ikz'} p(z', t), \end{aligned} \quad (18b)$$

$$\frac{\partial}{\partial t} p = -\gamma_{\perp} [(1 + i\delta_0) p - d(e^{ikz} Y_F + e^{-ikz} Y_B)], \quad (18c)$$

$$\frac{\partial}{\partial t} d = -\gamma_{\parallel} (d - d^{eq}) - \frac{1}{2} \gamma_{\parallel} [p^*(e^{ikz} Y_F + e^{-ikz} Y_B) + \text{c.c.}], \quad (18d)$$

where $\kappa = cT/\Lambda$ denotes the field damping rate out of the cavity. Note that $d^{eq} = -1$ for an absorbing medium.

The boundary conditions (12) are consistent with the following expansion of the field amplitudes in terms of the cavity modes:

$$Y_F(z, t) = \sum_{n=-\infty}^{+\infty} f_n(t) e^{i2n\pi z/\Lambda}, \quad (19a)$$

$$Y_B(z, t) = \sum_{n=-\infty}^{+\infty} b_n(t) e^{-i2n\pi z/\Lambda}. \quad (19b)$$

In this way, the partial differential equations (18a) and (18b) become an infinite collection of ordinary differential equations for the modal amplitudes $f_n(t)$ and $b_n(t)$ ($-\infty < n < +\infty$). In the uniform-field limit [Eqs. (16) and (17)] the intermode spacing is much larger than the width of each cavity mode κ , while the cavity mistuning δ_c is of the order of κ . This implies that the injected field is almost resonant with only one cavity mode (the one labeled $n=0$), and that all the other modes can be ignored if they are initially unexcited and if they are not affected by dynamical instabilities. These are not expected to emerge if the atomic linewidth γ_{\perp} is sufficiently smaller than the intermode spacing.

On the basis of these observations, we project the field equations (18a) and (18b) onto the $n=0$ modes and ignore all modes with indices $n \neq 0$ in the atomic equations (18c) and (18d) with the result

$$\frac{d}{d\tau} f(\tau) = -\tilde{\kappa}(1 + i\theta) f + \tilde{\kappa} Y_I + \tilde{\kappa} 2C \frac{1}{L} \int_0^L dz' e^{-ikz'} p(z', \tau), \quad (20a)$$

$$\frac{d}{d\tau} b(\tau) = -\tilde{\kappa}(1 + i\theta) b + \tilde{\kappa} 2C \frac{1}{L} \int_0^L dz' e^{ikz'} p(z', \tau), \quad (20b)$$

$$\frac{d}{d\tau} p(z, \tau) = -(1 + i\delta_0) p + d(e^{ikz} f + e^{-ikz} b), \quad (20c)$$

$$\frac{d}{d\tau} d(z, \tau) = -\gamma(d - d^{eq}) - \frac{1}{2} \gamma [p^*(e^{ikz} f + e^{-ikz} b) + \text{c.c.}], \quad (20d)$$

where $f(\tau) \equiv f_0(\tau)$, $b(\tau) \equiv b_0(\tau)$, $\tau = \gamma_{\perp} t$, $\tilde{\kappa} = \kappa/\gamma_{\perp}$, and $\gamma = \gamma_{\parallel}/\gamma_{\perp}$. In arriving at Eqs. (20a) and (20b) we have used the approximate equality

$$\int_0^{\Lambda} dz \frac{1}{\lambda} \int_z^{z+\lambda} dz' e^{\pm ikz'} p(z', t) \approx \int_0^L dz' e^{\pm ikz'} p(z', \tau), \quad (21)$$

which holds if $L \gg \lambda$, and if the atomic polarization vanishes outside the domain $0 \leq z \leq L$. Note that, in writing Eqs. (20c) and (20d), we have changed the partial time derivative into an ordinary time derivative because from now on z is just a label, instead of an independent variable.

For the purpose of our subsequent analyses, and in particular the numerical computations, it is convenient to avoid the continuous label z . This is made possible by defining the atomic ‘‘modal’’ amplitudes

$$p_m(\tau) = \frac{1}{L} \int_0^L dz e^{-imkz} p(z, \tau), \quad (22a)$$

$$d_m(\tau) = \frac{1}{L} \int_0^L dz e^{-imkz} d(z, \tau). \quad (22b)$$

where $m = 0, \pm 1, \pm 2, \dots$, and $d_m^* = d_{-m}$ because $d(z, \tau)$ is real. It then follows from Eqs. (20) and (22) that

$$\frac{d}{d\tau} f = -\tilde{\kappa}[(1+i\theta)f - Y_I - 2Cp_1], \quad (23a)$$

$$\frac{d}{d\tau} b = -\tilde{\kappa}[(1+i\theta)b - 2Cp_{-1}], \quad (23b)$$

$$\frac{d}{d\tau} p_m = -(1+i\delta_0)p_m + (d_{m-1}f + d_{m+1}b), \quad (23c)$$

$$\begin{aligned} \frac{d}{d\tau} d_m = & -\gamma(d_m - d^{eq}\delta_{m,0}) - \frac{1}{2}\gamma(p_{-(m-1)}^*f + p_{-(m+1)}^*b) \\ & - \frac{1}{2}\gamma(p_{m+1}f^* + p_{m-1}b^*), \end{aligned} \quad (23d)$$

Note that, when $b = 0$, Eqs. (23) reduce to the much simpler equations for a unidirectional ring resonator where the only nonzero atomic amplitudes are p_1 and d_0 .

The modal equations (23), which are equivalent to Eqs. (20), form the basis of our model for a bidirectional ring resonator with an injected field in the case when the medium is homogeneously broadened and the conditions for the UFL are satisfied. Although the model applies equally well to the description of a medium with gain, in the following we will focus only on the behavior of an absorbing system, i.e., on the case when $d^{eq} = -1$.

III. STEADY STATES

We now consider the matter of the possible steady states of Eqs. (23). Intuitively one might expect that, if nontrivial steady state solutions were to exist, the forward and backward fields would have to be synchronized in frequency. As it turns out, this is not possible for the case of an absorbing sample of atoms, as we show in this section. It is convenient to separate the discussion into two subsections, the first dealing with synchronous solutions, and the second concerned with the more general situation where the backward field and

the atomic variables (with the exception of d_0) develop frequency shifts with respect to the external driving field.

A. Synchronous steady state solutions

As we can see by direct inspection of Eqs. (23), the forward and backward modal amplitudes, f_{st} and b_{st} , are directly coupled to the polarization modes p_1 and p_{-1} , respectively, and indirectly to the remaining polarization variables characterized by odd indices and to the population variables carrying even indices. Thus, it follows that the possible synchronous steady states are solutions of the algebraic equations:

$$(1+i\theta)f_{st} - Y_I - 2Cp_1^{st} = 0, \quad (24a)$$

$$(1+i\theta)b_{st} - 2Cp_{-1}^{st} = 0, \quad (24b)$$

$$-(1+i\delta_0)p_{2m-1}^{st} + d_{2m-2}^{st}f_{st} + d_{2m}^{st}b_{st} = 0, \quad (24c)$$

$$\begin{aligned} d_{2m}^{st} - d^{eq}\delta_{m,0} + \frac{1}{2}(p_{-(2m-1)}^{st*}f_{st} + p_{-(2m+1)}^{st*}b_{st}) \\ + \frac{1}{2}(p_{2m+1}^{st}f_{st}^* + p_{2m-1}^{st}b_{st}^*) = 0, \end{aligned} \quad (24d)$$

where st denotes the stationary value of the corresponding variable. From Eq. (24c) we also have

$$p_{2m-1}^{st} = \frac{d_{2m-2}^{st}f_{st} + d_{2m}^{st}b_{st}}{1+i\delta_0}. \quad (25)$$

After substituting Eq. (25) into Eq. (24d) and keeping in mind that $d_m^* = d_{-m}$, we obtain the recursion relation

$$\xi d_{2m-2}^{st} + \eta d_{2m}^{st} + \xi^* d_{2m+2}^{st} = d^{eq}\delta_{m,0}, \quad (26)$$

where $m = 0, \pm 1, \pm 2, \dots$, and

$$\xi = \frac{f_{st}b_{st}^*}{1+\delta_0^2}, \quad (27a)$$

$$\eta = 1 + \frac{|f_{st}|^2 + |b_{st}|^2}{1+\delta_0^2}. \quad (27b)$$

In connection with Eq. (26), we distinguish two possibilities: $\xi = 0$, or $\xi \neq 0$. In the former case (i.e., for $b_{st} = 0$), Eq. (27b) yields

$$\eta = 1 + \frac{|f_{st}|^2}{1+\delta_0^2}, \quad (28)$$

and Eq. (26) reduces to

$$d_{2m}^{st} = \frac{1}{\eta} d^{eq}\delta_{m,0}. \quad (29)$$

Thus, Eq. (25) implies that

$$p_1^{st} = \frac{f_{st}d_0^{st}}{1+i\delta_0} = \frac{f_{st}}{1+i\delta_0} \frac{1}{\eta} d^{eq}, \quad (30a)$$

$$p_{-1}^{st} = 0, \quad (30b)$$

and, in turn, Eq. (30a), together with Eq. (24a), yields the steady-state equation

$$\left[\left(1 - \frac{2C d^{eq}}{1 + \delta_0^2 + |f_{st}|^2} \right) + i \left(\theta + \frac{2C \delta_0 d^{eq}}{1 + \delta_0^2 + |f_{st}|^2} \right) \right] f_{st} = Y_I \quad (31)$$

for the forward field amplitude. This is the familiar steady state bistability equation for a unidirectional ring resonator [4].

If $\xi \neq 0$, then from Eq. (27a) it follows that the backward field b_{st} is not equal to zero and we have to solve the recursion relation (26), which can be written explicitly in the form

$$\xi d_{-2}^{st} + \eta d_0^{st} + \xi^* d_2^{st} = d^{eq} \quad (m=0), \quad (32a)$$

$$\xi d_0^{st} + \eta d_2^{st} + \xi^* d_4^{st} = 0 \quad (m=1), \quad (32b)$$

$$\xi d_2^{st} + \eta d_4^{st} + \xi^* d_6^{st} = 0 \quad (m=2), \quad (32c)$$

...

plus the complex conjugates of Eqs. (32b), (32c), etc.

Next, we note that Eq. (32b) can also be written as

$$\xi^* \frac{d_2^{st}}{d_0^{st}} = - \frac{|\xi|^2}{\eta + \xi^* \frac{d_4^{st}}{d_2^{st}}}, \quad (33)$$

while Eq. (32c) yields,

$$\xi^* \frac{d_4^{st}}{d_2^{st}} = - \frac{|\xi|^2}{\eta + \xi^* \frac{d_6^{st}}{d_4^{st}}}, \quad (34)$$

etc. These results imply,

$$\xi^* \frac{d_2^{st}}{d_0^{st}} = \xi^* \frac{d_4^{st}}{d_2^{st}} = \dots = - \frac{|\xi|^2}{\eta - \frac{|\xi|^2}{\eta - \dots}} = - \frac{|\xi|^2}{\eta + \xi^* \frac{d_2^{st}}{d_0^{st}}}. \quad (35)$$

Consider now the quadratic equation

$$\xi^* \frac{d_2^{st}}{d_0^{st}} = - \frac{|\xi|^2}{\eta + \xi^* \frac{d_2^{st}}{d_0^{st}}}, \quad (36)$$

whose roots are

$$\left(\xi^* \frac{d_2^{st}}{d_0^{st}} \right)_{\pm} = \frac{1}{2} \left(-\eta \pm \sqrt{\eta^2 - 4|\xi|^2} \right) = \left(\xi^* \frac{d_4^{st}}{d_2^{st}} \right)_{\pm} = \dots, \quad (37)$$

where

$$\eta^2 - 4|\xi|^2 = 1 + \left(\frac{|f_{st}|^2 - |b_{st}|^2}{1 + \delta_0^2} \right)^2 + 2 \frac{|f_{st}|^2 + |b_{st}|^2}{1 + \delta_0^2}. \quad (38)$$

A simple analysis of the roots of Eq. (36) shows that the root labeled $(\dots)_-$ yields

$$\left| \frac{d_2^{st}}{d_0^{st}} \right| > 1, \quad (39a)$$

leading to the unphysical result $|d_{2m}^{st}| \rightarrow \infty$ as $m \rightarrow \infty$. The second root, instead, is consistent with the ratio

$$\left| \frac{d_2^{st}}{d_0^{st}} \right| < 1, \quad (39b)$$

as it must be. By combining Eq. (37) with Eq. (32a) we can calculate each d_{2m}^{st} . In particular, we have

$$d_0^{st} = \frac{d^{eq}}{\sqrt{\eta^2 - 4|\xi|^2}}, \quad (40a)$$

$$d_{-2}^{st} = \frac{d^{eq}}{2\xi} \left(1 - \frac{\eta}{\sqrt{\eta^2 - 4|\xi|^2}} \right), \quad (40b)$$

and thus, according to Eq. (25), we have

$$\begin{aligned} p_{-1}^{st} &= \frac{d_{-2}^{st} f_{st} + d_0^{st} b_{st}}{1 + i\delta_0} \\ &= (1 - i\delta_0) \frac{d^{eq}}{2|b_{st}|^2} \left(1 - \frac{\eta - 2|b_{st}|^2/(1 + \delta_0^2)}{\sqrt{\eta^2 - 4|\xi|^2}} \right) b_{st}. \end{aligned} \quad (41)$$

It follows, from Eqs. (24b) and (41), that

$$\theta = -\delta_0, \quad (42a)$$

$$2|b_{st}|^2 = 2C d^{eq} \left(1 - \frac{\eta - 2|b_{st}|^2/(1 + \delta_0^2)}{\sqrt{\eta^2 - 4|\xi|^2}} \right). \quad (42b)$$

It is easy to show that

$$1 - \frac{\eta - 2|b_{st}|^2/(1 + \delta_0^2)}{\sqrt{\eta^2 - 4|\xi|^2}} > 0. \quad (43)$$

so that, for an absorbing medium ($d^{eq} < 0$), Eq. (42b) can never be satisfied. Thus, no steady state is possible for $\xi \neq 0$, and the only synchronous stationary solutions are those whose backward field amplitude is equal to zero. This conclusion was also reached by Asquini and Casagrande [7] under resonance conditions but without invoking the uniform field limit.

B. Nonsynchronous steady states

Somewhat unexpectedly, Eqs. (23) admit a class of long-time solutions in which the backward field and the atomic modal variables (with the exception of d_0) oscillate with a frequency that is different from that of the driving field. More precisely, we seek long-time solutions of the form,

$$f(\tau) = f_{st}, \quad (44a)$$

$$b(\tau) = b_{st} e^{-i\Delta\tau}, \quad (44b)$$

$$p_{2m-1}(\tau) = p_{2m-1}^{st} e^{i(m-1)\Delta\tau}, \quad (44c)$$

$$d_{2m}(\tau) = d_{2m}^{st} e^{im\Delta\tau}, \quad (44d)$$

where Δ is an unknown frequency shift (measured in units of γ_{\perp}) and $f_{st}, b_{st}, p_{2m-1}^{st}, d_{2m}^{st}$ are all constant. If solutions of this type exist and are stable, direct experimental evidence could be provided by looking for a beat note between the forward and backward field components.

Substitution of the ansatz (44) into Eqs. (23) yields the following nonlinear algebraic set of equations:

$$(1 + i\theta)f_{st} - Y_I - 2Cp_1^{st} = 0, \quad (45a)$$

$$\left[1 + i \left(\theta - \frac{\Delta}{\kappa} \right) \right] b_{st} - 2Cp_{-1}^{st} = 0, \quad (45b)$$

$$-[1 + i(\delta_0 + m\Delta)]p_{2m-1}^{st} + d_{2m-2}^{st}f_{st} + d_{2m}^{st}b_{st} = 0, \quad (45c)$$

$$\begin{aligned} & \left(1 + im \frac{\Delta}{\gamma} \right) d_{2m}^{st} - d^{eq} \delta_{m,0} + \frac{1}{2} (p_{-(2m-1)}^{st*} f_{st} + p_{-(2m+1)}^{st*} b_{st}) \\ & + \frac{1}{2} (p_{2m+1}^{st} f_{st}^* + p_{2m-1}^{st} b_{st}^*) = 0, \end{aligned} \quad (45d)$$

for the unknown steady state amplitudes and frequency shift Δ [12], which we have solved using the globally convergent method of Ref. [13].

Note that, as $\tilde{\kappa}$ gets smaller for decreasing mirror transmittivity, Δ must also decrease so that the ratio $\Delta/\tilde{\kappa}$ in Eq. (45b) remains finite. We have checked the correctness of this plausible guess numerically. At the same time, it might appear that, for sufficiently small values of Δ and finite m , one might neglect the contributions $m\Delta$ in Eqs. (45c) and (45d). As it turns out, we have also verified that the maximum number of modes that must be kept for an accurate solution of Eqs. (45) increases as Δ decreases so that, apparently, these contributions are never negligible and, as a consequence, the continued fraction technique discussed in the previous section cannot be applied.

A typical example of possible steady state values for f_{st} and b_{st} is shown in Fig. 2 together with the well-known corresponding steady state of the forward field in ordinary optical bistability. As one can readily anticipate from these numerical solutions, not all steady-state values are accessible (just as the negative-slope segment of the stationary bistabil-

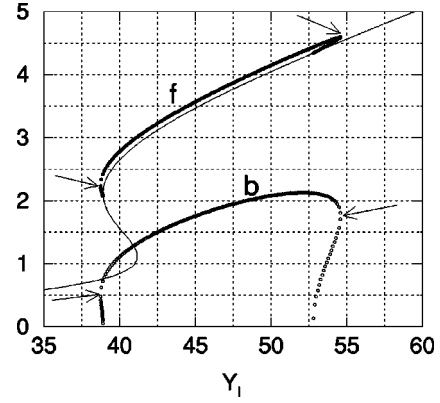


FIG. 2. The moduli of f_{st} and b_{st} (labeled f and b , respectively) are plotted as functions of the driving field amplitude Y_I together with the steady-state curve of unidirectional bistability (thin solid line). The parameters of this simulation are $\delta_0 = -0.1$, $\theta = -11.5$, $\gamma = 2$, $2C = 79$, $\tilde{\kappa} = 0.09$. The stationary solutions below the turning points (indicated by the arrows) satisfy Eqs. (45) but are not physically accessible because they are unstable.

ity curve is not accessible). We will return to this aspect of the problem in our discussion of the time-dependent solutions and their stability.

IV. TIME-DEPENDENT SOLUTIONS

In order to analyze the behavior of the system as a function of time, we have integrated Eqs. (23) using a standard Runge-Kutta method with adaptive-step-size control. These equations involve an infinite hierarchy of atomic variables, but numerical tests have shown that, for a large range of parameters, a cutoff at $m = \pm 10$ is already sufficient for convergence of the solutions to a satisfactory level of accuracy. Because we are considering a homogeneously broadened absorbing medium, we have set $d^{eq} = -1$. In addition, we have selected Y_I to be real for definiteness. A natural choice of initial conditions is such that every dependent variable begins at zero, except for d_0 that is real and initially equal to -1 . Furthermore, we have assigned a small initial value to the backward field [typically such that $|b(\tau=0)| = 1.0 \times 10^{-4}$] to simulate the spontaneous emission noise of the system.

Our analysis of the previous section has shown the possibility that long-time solutions of Eqs. (23) with a nonzero backward field may take the form (44) with a frequency shift Δ between the oscillation frequencies of the backward and forward fields. Our numerical simulations have shown that $b(\tau)$ may vanish, in spite of the initial nonzero value of this variable and, if so, the solution approaches the steady-state configuration of the unidirectional ring resonator. However, for a wide range of parameter values, this type of solution becomes unstable, and the field and atomic variables evolve into the general form given by Eqs. (44).

In this case, a typical early stage of the evolution of the fields is shown in Fig. 3. For the chosen parameters, the modulus of the backward field grows monotonically, and eventually reaches a constant value in approximately 1200

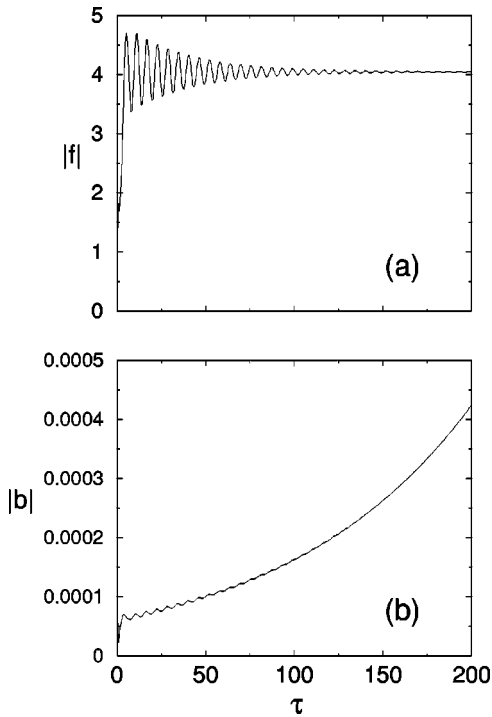


FIG. 3. The early time-dependent evolution of the moduli of the forward (a) and backward (b) cavity fields, corresponding to $Y_I = 50$. The remaining parameters of this simulation are $\delta_0 = -0.1$, $\theta = -11.5$, $\gamma = 2$, $2C = 79$, $\tilde{\kappa} = 0.09$.

units of the dimensionless time τ . At this point, the real and imaginary parts of the forward field f_{st} are constant (not shown), but the real and imaginary parts of $b(\tau)$ undergo sinusoidal oscillations with constant amplitude, as shown in Fig. 4. These results show clearly that, after a sufficiently long time, the forward field reaches a steady state and that it oscillates with the frequency of the external field, while the backward field, which is also in steady state, oscillates with a frequency shifted by an amount Δ , whose magnitude can be extracted from the data shown in Fig. 4.

Figure 5 shows a collection of values of $|f_{st}|$ and $|b_{st}|$

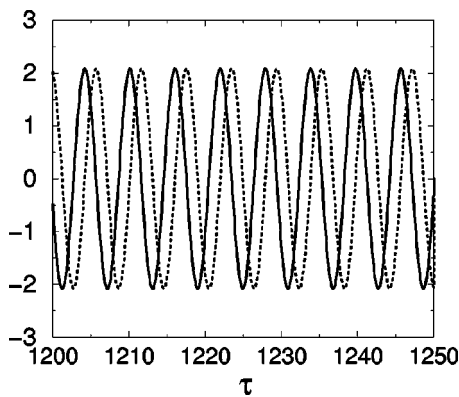


FIG. 4. Long-time behavior of the real part (solid line) and imaginary part (dotted line) of the backward field for the same parameters adopted in Fig. 3. Because the forward field is constant, over the same time range, the oscillations of the backward field display the nonsynchronous nature of the solution.

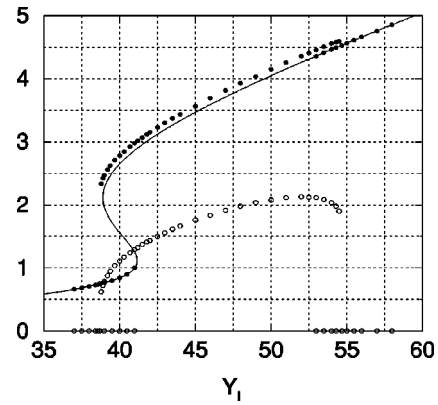


FIG. 5. The moduli of f_{st} (solid circles) and b_{st} (open circles) are plotted as functions of the driving field amplitude Y_I together with the steady state curve of unidirectional bistability (thin solid line). The accessible steady-state values, obtained by the numerical solution of Eqs. (23), are in excellent agreement with the corresponding solutions of the stationary equations (45). The parameters of this simulation are $\delta_0 = -0.1$, $\theta = -11.5$, $\gamma = 2$, $2C = 79$, $\tilde{\kappa} = 0.09$.

obtained by varying the injected field amplitude Y_I , together with a solid line representing the modulus of the forward field for a unidirectional ring resonator. We obtained these results by starting the first run at the value $Y_I = 37$ with the initial conditions described above, and continuing the time integration until the moduli of f and b became constant. At this point we increased Y_I and repeated the procedure, with the final values of the earlier run chosen as the new initial conditions.

For the assigned parameters, our numerical solutions show that b continues to be zero and $|f_{st}|$ varies along the lower branch of the bistability state equation until Y_I reaches the approximate value of 41.2 (see Fig. 5). At this point the forward field “jumps up,” as it would in a unidirectional ring resonator, and the backward field acquires a nonzero magnitude for the first time. Note, however, that the forward field lands well above the upper branch of the unidirectional bistability curve. After this jump, both fields vary continuously, as we change Y_I , until we reach approximately $Y_I = 54.6$ where $|b_{st}|$ becomes equal to zero and $|f_{st}|$ approaches the upper branch of the bistability state equation.

Upon decreasing Y_I , the situation does not change until $Y_I = 52.7$ where $|b_{st}|$ becomes finite and $|f_{st}|$, correspondingly, moves away from the bistability steady state curve. When Y_I approaches the approximate value 38.7, the forward field jumps down back to the lower branch of the state equation and the backward field vanishes. So, hysteresis manifests itself for both fields, at both ends of a finite range of values of the injected field amplitude.

We should also point out that sudden jumps and hysteresis are not always present when the backward field develops a nonzero stationary value. Figure 6 was constructed in the same way as Fig. 5, but for different values of the parameters. Here both fields vary continuously, as Y_I changes, and again the backward field acquires a nonzero magnitude inside a bounded range of values of Y_I . Note that, although the

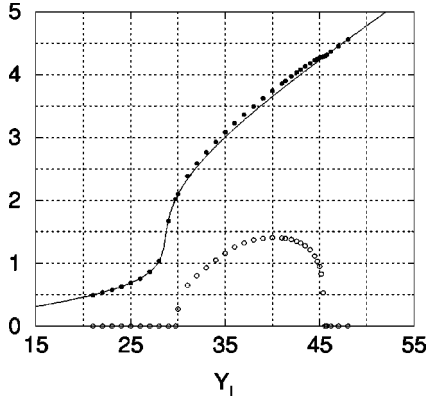


FIG. 6. The moduli of f_{st} (solid circles) and b_{st} (open circles) are plotted as functions of the driving field amplitude Y_I together with the steady-state curve of unidirectional bistability (thin solid line). The parameters used in this simulation are $\delta_0=0$, $\theta=-10$, $\gamma=2$, $2C=50$, $\tilde{\kappa}=0.2$.

cavity-damping rate $\tilde{\kappa}$ does not affect the steady-state behavior of the forward field in unidirectional bistability, it does play a role in determining the existence and stability of the nonzero backward field solutions in the case of a bidirectional ring resonator [see Eqs. (45)].

Stationary behaviors are not the only possible outcomes of the long-time dynamics. We have seen instances in which forward and backward fields coexist and undergo self-pulsing oscillations. However, we have chosen not to investigate this aspect of the problem.

It is interesting, instead, to display the population difference $d(z, \tau)$ as a function of z . In terms of the population modal amplitudes, this variable is given by

$$d(z, \tau) = \sum_m d_{2m}(\tau) e^{i2mkz}. \quad (46)$$

Figure 7 shows how the population difference varies with kz at a selected time $\tau = \tau_1$ (solid line) after all transients have died out, and at a slightly later time $\tau = \tau_1 + 1.22$ (dotted line). This behavior suggests the existence of a moving-

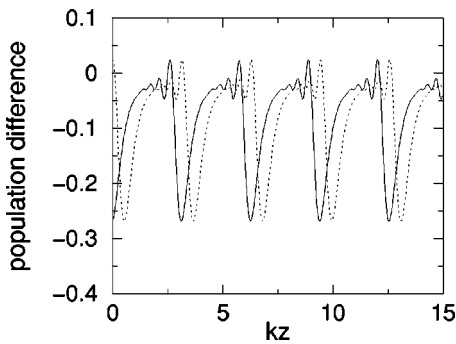


FIG. 7. Spatial profile of the population difference plotted as a function of kz after a long time τ_1 (solid line) and at the slightly later time $\tau_1 + 1.22$ (dotted line) for a value of the driving field amplitude $Y_I=50$. The remaining parameters of this simulation are $\delta_0=-0.1$, $\theta=-11.5$, $\gamma=2$, $2C=79$, $\tilde{\kappa}=0.09$.

spatial grating in the population difference. Perhaps the most notable feature is that, although the spatial average of the population difference is negative, periodically there are regions where the population difference is greater than zero and, thus, these regions have gain.

V. LINEAR STABILITY ANALYSIS

It is already known from previous studies [4,11] that the steady-state solutions of unidirectional bistability may become unstable along a segment of the upper branch and give way to self-oscillations. Asquini and Casagrande [7] generalized the studies of Ref. [11] for the case of a bidirectional ring cavity under resonant conditions. Here we complete the development of our previous sections and extend the treatment of Ref. [7] by carrying out a linear-stability analysis for arbitrary values of the detuning parameters. In particular, we associate the appearance of solutions having a nonzero backward field with the instability of the trivial solution under infinitesimal perturbations, where by ‘‘trivial solution’’ we mean a configuration where f_{st} obeys Eq. (31), where

$$d_0^{st} = \frac{(1 + \delta_0^2) d^{eq}}{1 + \delta_0^2 + |f_{st}|^2}, \quad (47a)$$

$$p_1^{st} = \frac{d_0^{st} f_{st}}{1 + i\delta_0}, \quad (47b)$$

and b and the other modal components vanish.

The linearized form of Eqs. (23) around an arbitrary-trivial state is given by

$$\frac{d}{d\tau} \delta f = -\tilde{\kappa}(1 + i\theta) \delta f + \tilde{\kappa} 2C \delta p_1, \quad (48a)$$

$$\frac{d}{d\tau} \delta b = -\tilde{\kappa}(1 + i\theta) \delta b + \tilde{\kappa} 2C \delta p_{-1}, \quad (48b)$$

$$\begin{aligned} \frac{d}{d\tau} \delta p_{2m-1} = & -(1 + i\delta_0) \delta p_{2m-1} + f_{st} \delta d_{2m-2} \\ & + d_0^{st} \delta_{m,1} \delta f + d_0^{st} \delta_{m,0} \delta b, \end{aligned} \quad (48c)$$

$$\begin{aligned} \frac{d}{d\tau} \delta d_{2m} = & -\gamma \delta d_{2m} - \frac{1}{2} \gamma (f_{st} \delta p_{-(2m-1)}^* + p_1^{st*} \delta_{m,0} \delta f \\ & + p_1^{st*} \delta_{m,-1} \delta b) - \frac{1}{2} \gamma (f_{st}^* \delta p_{2m+1} \\ & + p_1^{st} \delta_{m,0} \delta f^* + p_1^{st} \delta_{m,1} \delta b^*), \end{aligned} \quad (48d)$$

together with their complex conjugates. In Eqs. (48), δf , δb , δp_{2m-1} , and δd_{2m} , for $m=0, \pm 1, \pm 2, \dots$, denote the deviations from the respective steady-state values of the variables.

By inspection, we see that Eqs. (48) split into three groups, each forming a closed set of equations. The first group includes,

$$\frac{d}{d\tau} \delta f = -\tilde{\kappa}(1+i\theta) \delta f + \tilde{\kappa} 2C \delta p_1, \quad (49a)$$

$$\frac{d}{d\tau} \delta f^* = -\tilde{\kappa}(1-i\theta) \delta f^* + \tilde{\kappa} 2C \delta p_1^*, \quad (49b)$$

$$\frac{d}{d\tau} \delta p_1 = -(1+i\delta_0) \delta p_1 + f_{st} \delta d_0 + d_0^{st} \delta f, \quad (49c)$$

$$\frac{d}{d\tau} \delta p_1^* = -(1-i\delta_0) \delta p_1^* + f_{st}^* \delta d_0 + d_0^{st} \delta f^*, \quad (49d)$$

$$\frac{d}{d\tau} \delta d_0 = -\gamma \delta d_0 - \frac{1}{2} \gamma (f_{st} \delta p_1^* + p_1^{st*} \delta f + f_{st}^* \delta p_1 + p_1^{st} \delta f^*), \quad (49e)$$

which we recognize as the linearized equations of unidirectional bistability. The second group couples the fluctuation variables δb , δp_{-1} , δd_{-2} , and δp_3^* according to

$$\frac{d}{d\tau} \delta b = -\tilde{\kappa}(1+i\theta) \delta b + \tilde{\kappa} 2C \delta p_{-1}, \quad (50a)$$

$$\frac{d}{d\tau} \delta p_{-1} = -(1+i\delta_0) \delta p_{-1} + f_{st} \delta d_{-2} + d_0^{st} \delta b, \quad (50b)$$

$$\frac{d}{d\tau} \delta d_{-2} = -\gamma \delta d_{-2} - \frac{1}{2} \gamma (f_{st} \delta p_3^* + p_1^{st*} \delta b + f_{st}^* \delta p_{-1}), \quad (50c)$$

$$\frac{d}{d\tau} \delta p_3^* = -(1-i\delta_0) \delta p_3^* + f_{st}^* \delta d_{-2}, \quad (50d)$$

where we have used the identity $d_2^* = d_{-2}$. The third group is comprised of an infinite set of triplets of equations of the form

$$\frac{d}{d\tau} \delta p_{-2n+1} = -(1+i\delta_0) \delta p_{-2n+1} + f_{st} \delta d_{-2n}, \quad (51a)$$

$$\frac{d}{d\tau} \delta d_{-2n} = -\gamma \delta d_{-2n} - \frac{1}{2} \gamma (f_{st} \delta p_{2n+1}^* + f_{st}^* \delta p_{-2n+1}), \quad (51b)$$

$$\frac{d}{d\tau} \delta p_{2n+1}^* = -(1-i\delta_0) \delta p_{2n+1}^* + f_{st}^* \delta d_{-2n}, \quad (51c)$$

where $n \neq 0, \pm 1$.

The eigenvalues of Eqs. (49) have already been analyzed in past studies of unidirectional bistability and self-pulsing [4]. The sets of Eqs. (50) and (51), instead, contain information on the possible emergence of solutions in which the backward field plays a dynamical role.

We consider first Eqs. (51) for an arbitrary value of the index n (with $n \neq 0, \pm 1$). The characteristic equation takes the form

$$\lambda^3 + (\gamma + 2)\lambda^2 + (1 + \delta_0^2 + 2\gamma + \gamma|f_{st}|^2)\lambda + \gamma(1 + \delta_0^2 + 2\gamma + \gamma|f_{st}|^2) = 0. \quad (52)$$

With the help of the Hurwitz criterion [14], it is easy to prove that all three roots of Eq. (52) have a negative real part, which implies that the only fluctuations that may be amplified and eventually destroy the trivial solution are governed by Eqs. (49) or (50) [and the complex conjugate of Eq. (50)].

Although the characteristic equation associated with Eqs. (49) is already known, for completeness we reproduce it below together with the characteristic equation (50). For Eqs. (49) we have,

$$\lambda^5 + c_4\lambda^4 + c_3\lambda^3 + c_2\lambda^2 + c_1\lambda + c_0 = 0 \quad (53)$$

and for Eqs. (50)

$$\lambda^4 + b_3\lambda^3 + b_2\lambda^2 + b_1\lambda + b_0 = 0, \quad (54)$$

where

$$c_4 = 2 + \gamma + 2\tilde{\kappa}, \quad (55a)$$

$$c_3 = 1 + \delta_0^2 + \gamma|f_{st}|^2 + 2\gamma + \tilde{\kappa}^2(1 + \theta^2) + 2\tilde{\kappa}(2 + \gamma) - 2\tilde{\kappa} 2C d_0^{st}, \quad (55b)$$

$$c_2 = \gamma(1 + \delta_0^2 + |f_{st}|^2) + 2\tilde{\kappa}(1 + 2\gamma + \delta_0^2 + \gamma|f_{st}|^2) + \tilde{\kappa}^2(2 + \gamma)(1 + \theta^2) - 2\tilde{\kappa} 2C d_0^{st} \left(1 + \tilde{\kappa} + \gamma - \frac{\gamma|f_{st}|^2}{2(1 + \delta_0^2)} \right), \quad (55c)$$

$$c_1 = 2\tilde{\kappa}\gamma(1 + \delta_0^2 + |f_{st}|^2) + \tilde{\kappa}^2(1 + 2\gamma + \delta_0^2 + \gamma|f_{st}|^2) + (\tilde{\kappa} 2C d_0^{st})^2 - 2\tilde{\kappa} 2C d_0^{st} \left[\gamma + \tilde{\kappa} \left(1 - \theta\delta_0 + \gamma - \frac{\gamma|f_{st}|^2(1 + \theta\delta_0)}{2(1 + \delta_0^2)} \right) \right], \quad (55d)$$

$$c_0 = \gamma\tilde{\kappa}^2(1 + \theta^2)(1 + \delta_0^2 + |f_{st}|^2) + (\tilde{\kappa} 2C d_0^{st})^2 \gamma \left(1 - \frac{|f_{st}|^2}{1 + \delta_0^2} \right) - 2\tilde{\kappa}^2 2C d_0^{st} \gamma(1 - \theta\delta_0), \quad (55e)$$

and

$$b_3 = 2 + \gamma + \tilde{\kappa}(1 + i\theta), \quad (56a)$$

$$b_2 = 1 + \delta_0^2 + \gamma|f_{st}|^2 + 2\gamma + \tilde{\kappa}(1 + i\theta)(2 + \gamma) - \tilde{\kappa} 2C d_0^{st}, \quad (56b)$$

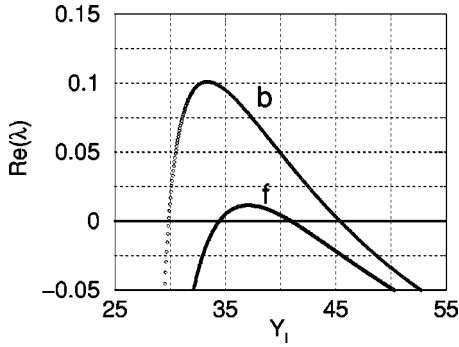


FIG. 8. The real parts of the solutions of the characteristic equations (54) (labeled b) and (53) (labeled f) are plotted as functions of the driving field amplitude Y_I for the parameters $\delta_0=0$, $\theta=-10$, $\gamma=2$, $2C=50$, $\tilde{\kappa}=0.2$.

$$b_1 = \gamma(1 + \delta_0^2 + |f_{st}|^2) + \tilde{\kappa}(1 + i\theta)(1 + 2\gamma + \delta_0^2 + \gamma|f_{st}|^2) - \tilde{\kappa}2Cd_0^{st} \left(1 + \gamma - i\delta_0 - \frac{\gamma|f_{st}|^2}{2(1 - i\delta_0)} \right), \quad (56c)$$

$$b_0 = \gamma\tilde{\kappa}(1 + i\theta)(1 + \delta_0^2 + |f_{st}|^2) - \tilde{\kappa}2Cd_0^{st}\gamma(1 - i\delta_0). \quad (56d)$$

We have obtained the roots of Eqs. (53) and (54) numerically. For the parameters chosen in the construction of Fig. 5 we find that, on the upper branch of the unidirectional bistability curve, one (and only one) of the roots of Eq. (54) has a positive real part in the range $38.8 < Y_I < 52.8$, while all roots of Eq. (53) have a negative real part. This is consistent with the observed behavior of the time-dependent equations (23) whose solutions evolve with a nonzero-backward field at $Y_I=52.7$, when Y_I is scanned in the direction of decreasing values. Incidentally, we note that the root with a positive real part has an imaginary part that is quite close to the frequency shift Δ calculated from the time-dependent solutions (see Sec. IV, Fig. 4).

The situation is more complicated (and interesting) for the parameters chosen in Fig. 6 because in this case both Eqs. (53) and (54) have one root having a positive real part for a range of values of Y_I [15]. As shown in Fig. 8 the ranges of instability overlap, in part, but have considerably different widths; in addition, the real parts of the unstable roots of Eq. (54) are significantly larger than those of the corresponding roots of Eq. (53). Similar behavior shows up for various parameter combinations and appears to be rather common.

If a driving field amplitude is chosen from within the common domain of instability, and if we artificially turn off the backward field and the appropriate atomic variables, the forward field will eventually evolve into a self-pulsing state, as it should. However, if we allow the cavity field to operate also in the backward direction, an arbitrarily small initial fluctuation of the backward field will grow, destroy the self-pulsing state and bring the entire system to a stationary state, as shown in Fig. 3. This behavior suggests that the self-pulsing state of unidirectional bistability is unstable in the bidirectional model (for the chosen parameters) and that the only attractor in this case is the stationary state with a

nonzero-backward field. The same outcome was observed by starting from an initial condition in which both forward and backward fields were zero and by applying a small initial perturbation to the backward field to simulate spontaneous emission noise.

In general, i.e., for different selections of the parameters, the situation appears to be more complicated because we also found instances in which the self-pulsing state (with $b_{st}=0$) and the nonsynchronous steady states behave as coexisting attractors. For example, in correspondence with the parameters $\delta_0=-0.1$, $\theta=-9.5$, $\gamma=2$, $2C=79$, and $\tilde{\kappa}=0.55$, both Eqs. (53) and (54) have one root having a positive real part in the range $40.2 < Y_I < 64.3$. If we select a value of the external driving field from within the common domain of instability, the system evolves into different attractors depending on the initial conditions. These coexisting attractors appear to be quite removed from each other, so that we never observed random switching between the two domains in response to small perturbations (e.g., numerical noise or artificially induced small jumps during the evolution).

In order to observe a stationary state with a nonzero value of the backward field, the best strategy, perhaps also viable experimentally, might be to observe that the domain of instability of the backward field is broader than that of the forward field, and to select a value of the driving field for which only the backward field is unstable. This should promote the evolution of the system into a long-time stationary state of the type described by Eq. (44).

VI. SUMMARY AND CONCLUSIONS

In this paper we have explored the influence of the backward mode of propagation of the cavity field on the dynamics of a ring resonator driven by an external field and containing an ensemble of absorbing two-level atoms. After developing a first-principles description of this problem in the plane wave and semiclassical approximations, we have derived the working equations in the uniform field limit. These equations describe the coupled evolution of the forward and backward cavity field amplitudes and of an infinite hierarchy of atomic ‘‘modal’’ variables.

The main result of our analysis is the prediction of a steady-state configuration in which the forward and backward fields have constant amplitudes but different frequencies of oscillation. This prediction is supported by the long-time behavior of the equations of motion and is further confirmed by two additional independent calculations. The first is based on the solution of a nonlinear system of algebraic equations for the steady-state values of the variables, and the second is the analysis of the linear response of the system in the neighborhood of a unidirectional steady state.

The linear-stability analysis also shows that, at least for the parameters adopted in this study, the unidirectional steady state can become unstable against the growth of a backward wave over a domain that is significantly wider than that over which self-pulsing of the forward field is predicted to emerge. Thus, appropriate values of the parameters can be

selected that can lead to the observation of a stationary-backward field without dynamical competition from the self-pulsing state. Under these conditions, if one overlaps the forward- and backward-output field, one should be able to observe a beat note at a frequency that we estimate should be of the order of the atomic polarization relaxation rate.

ACKNOWLEDGMENTS

We are greatly indebted to Professor M. Brambilla, Professor G. L. Lippi, Professor L. A. Lugiato, Professor G. L. Oppo, and Professor J. R. Tredicce for many useful remarks and illuminating comments.

-
- [1] For an early study of bidirectional emission from a laser-ring cavity, see P. Mandel and G. P. Agrawal, *Opt. Commun.* **42**, 269 (1982).
- [2] See, for example, H. Zeghlache, P. Mandel, N. B. Abraham, L.M. Hoffer, G.L. Lippi, and T. Mello, *Phys. Rev. A* **37**, 470 (1988), and references therein. See also N. B. Abraham, P. Mandel, and L. M. Narducci, in *Progress in Optics*, edited by E. Wolf (Elsevier, Amsterdam, 1988), Vol. XXV, p. 1; bidirectional ring lasers are reviewed on p. 153.
- [3] P. Meystre, *Opt. Commun.* **26**, 277 (1978); H. M. Gibbs, *Optical Bistability: Controlling Light with Light* (Academic Press, Orlando, 1985), see, for example, p. 46.
- [4] L. A. Lugiato, in *Progress in Optics*, edited by E. Wolf (Elsevier, Amsterdam, 1984), Vol. XXI, p. 69.
- [5] A. T. Rosenberger, L. A. Orozco, and H. J. Kimble, *Phys. Rev. A* **28**, R2569 (1983); L. A. Orozco, H. J. Kimble, and A. T. Rosenberger, *Opt. Commun.* **62**, 53 (1987); L. A. Orozco, A. T. Rosenberger, and H. J. Kimble, *Phys. Rev. A* **36**, 3248 (1987); *Phys. Rev. Lett.* **53**, 2547 (1984).
- [6] L. A. Orozco, H. J. Kimble, A. T. Rosenberger, L. A. Lugiato, M. L. Asquini, M. Brambilla, and L. M. Narducci, *Phys. Rev. A* **39**, 1235 (1989), see especially Sec. V E, p. 1250.
- [7] M. L. Asquini and F. Casagrande, *Z. Phys. B: Condens. Matter* **44**, 233 (1981).
- [8] The forward direction is identified as the direction of propagation of the external field.
- [9] L. A. Lugiato and L. M. Narducci, *Z. Phys. B: Condens. Matter* **71**, 129 (1988).
- [10] R. Bonifacio and L. A. Lugiato, *Lett. Nuovo Cimento Soc. Ital. Fis.* **21**, 505 (1978).
- [11] R. Bonifacio and L. A. Lugiato, *Lett. Nuovo Cimento Soc. Ital. Fis.* **21**, 510 (1978).
- [12] The number of equations (45), after suitable truncation to a maximum value of the index m , matches the number of unknowns, as the phase of the backward field is indeterminate and b_{st} can be selected to be real without loss of generality.
- [13] W. H. Press, B. P. Flannery, S. A. Teukolsky, and W. T. Vetterling, *Numerical Recipes in C*, 2nd ed. (Cambridge University Press, Cambridge, 1992), Chap. 9.7.
- [14] H. Haken, *Synergetics—An Introduction*, 3rd ed. (Springer, Heidelberg, 1983), p. 123.
- [15] To be more precise, Eq. (53) has two roots with the same positive real part; these roots are complex conjugate of each other.